Diagnostic Accuracy Study

Medicine®

OPEN

Differentiation between orbital malignant and benign tumors using intravoxel incoherent motion diffusion-weighted imaging

Correlation with dynamic contrast-enhanced magnetic resonance imaging

Xiao-Quan Xu, MD[a], Hao Hu, MD[a], Guo-Yi Su, MD[a], Hu Liu, MD, PhD[b], Fei-Yun Wu, MD, PhD[a,*], Hai-Bin Shi, MD, PhD[a,*]

Abstract

To evaluate the performance of intravoxel incoherent motion (IVIM) diffusion-weighted imaging (DWI) for differentiating orbital malignant from benign tumors, and to assess the correlation between IVIM-DWI parameters and dynamic contrast-enhanced magnetic resonance imaging (DCE-MRI) parameters.

Twenty-seven patients (17 benign and 10 malignant) with orbital tumors underwent 3.0T MRI examination for pre-treatment evaluation, including IVIM-DWI and DCE-MRI. IVIM-DWI parameters (tissue diffusivity, D; pseudo-diffusion coefficient, D^*; and perfusion fraction, f) were quantified using bi-exponential fitting model. DCE-MRI parameters (K^{trans}, the volume transfer constant between the plasma and the extracellular extravascular space [EES]; V_e, the volume fraction of the EES, and K_{ep}, the rate constant from EES to blood plasma) were quantified using modified Tofts model. Independent-sample *t* test, receiver operating characteristic curve analyses and Spearman correlation test were used for statistical analyses.

Malignant orbital tumors showed lower D ($P < .001$) and higher D^* ($P = .002$) than benign tumors. Setting a D value of 0.966×10^{-3} mm^2/s as the cut-off value, a diagnostic performance (AUC, 0.888; sensitivity, 100%; specificity, 82.35%) could be obtained for diagnosing malignant tumors. While setting a D^* value of 42.371×10^{-3} mm^2/s as cut-off value, a diagnostic performance could be achieved (AUC, 0.847; sensitivity, 90.00%; specificity, 70.59%). Poor or moderated correlations were found between IVIM-DWI and DCE-MRI parameters (D^* and K_{ep}, $r = 0.427$, $P = .027$; D and V_e, $r = 0.626$, $P < .001$).

IVIM-DWI is potentially useful for differentiating orbital malignant from benign tumors. Poor or moderate correlations exist between IVIM-DWI and DCE-MRI parameters. IVIM-DWI may be a useful adjunctive perfusion technique for the differential diagnosis of orbital tumors.

Abbreviations: AIF = arterial input function, DCE-MRI = dynamic contrast-enhanced magnetic resonance imaging, DWI = diffusion-weighted imaging, EES = extracellular extravascular space, ICC = intra-class correlation coefficient, IVIM = intravoxel incoherent motion, ROC = receiver operating characteristic, ROI = regions of interest.

Keywords: correlation, diffusion-weighted imaging, dynamic contrast-enhanced magnetic resonance imaging, intravoxel incoherent motion, orbital tumor

1. Introduction

Accurate differentiation between benign and malignant orbital tumors is very crucial for the determination of individual treatment.[1] Previously, conventional magnetic resonance imaging (MRI) features and diffusion-weighted imaging (DWI) were usually used for differentiating malignant from benign orbital tumors.[2–4] And, the ability of differentiation can be improved by combining with dynamic contrast-enhanced MRI (DCE-MRI).[5–7] DCE-MRI can supply supplemental information on the tumor perfusion and vessel permeability, by means of serial MRI scans taken before and after the intravenous injection of contrast agent.[8] However, contrast agent used in DCE-MRI scan can induce a severe adverse reaction in particular patients, such as those with renal dysfunction or allergies to contrast agent.[9]

Intravoxel incoherent motion (IVIM) DWI, firstly introduced by Le Bihan et al, allows for the separate analysis of pure molecular diffusion and microcirculation perfusion by analyzing the signal decay curve obtained from multiple b-value images with a bi-exponential model, and without need of contrast agent.[9] Previously, several studies demonstrated that IVIM-DWI could assist in differentiating different tumors and predicting disease prognosis in head and neck region.[10–12] Till now, only 1 study by Lecler et al applied IVIM-DWI in the field of orbital imaging, however, they focused on the repeatability of IVIM-DWI.[13] The study that using IVIM-DWI for differentiating orbital malignant

Editor: Neeraj Lalwani.

The authors have no conflicts of interest to disclose.

[a] Department of Radiology, [b] Department of Ophthalmology, The First Affiliated Hospital of Nanjing Medical University, Nanjing, Jiangsu, China.

[*] Correspondence: Hai-Bin Shi, Department of Radiology, The First Affiliated Hospital of Nanjing Medical University, No. 300, Guangzhou Rd., Nanjing, China (e-mail: shihb@njmu.edu.cn); Fei-Yun Wu, Department of Radiology, The First Affiliated Hospital of Nanjing Medical University, No. 300, Guangzhou Rd., Nanjing, China (e-mail: wfy_njmu@163.com).

Medicine (2019) 98:12(e14897)

Received: 5 October 2018 / Received in final form: 20 February 2019 / Accepted: 21 February 2019

http://dx.doi.org/10.1097/MD.0000000000014897

from benign tumors is lacked until now. In addition, whether IVIM-DWI correlated significantly with DCE-MRI is on debate. Conflicting results range from no correlation to moderate or strong correction in previous studies with application on hepatocellular carcinoma,[14] breast lesions,[15] soft tissue tumors,[16] lung cancer,[17] and head and neck tumors.[9,18,19]

Therefore, the purpose of this study was to evaluate the value of IVIM-DWI for differentiating orbital malignant from benign tumors, and to assess the correlation between IVIM-DWI derived parameters and the perfusion metrics obtained from DCE-MRI in orbital tumors.

2. Methods

2.1. Subjects

Our retrospective study protocol was reviewed and approved by the institutional review board of our hospital. Requirement for written informed consent was waived due to the retrospective nature of the analysis. Between May 2017 and October 2017, 41 consecutive patients with orbital tumors underwent MRI examination for pre-treatment evaluation. We excluded 14 patients according to the following exclusion criteria:

1) either IVIM-DWI or DCE-MRI was not performed (n = 6);
2) the diagnosis was not confirmed by pathological examination (n = 4);
3) prior chemotherapy or radiation therapy was performed before MRI examination (n = 2);
4) the image quality was not adequate for further imaging analysis (n = 2).

Finally, a total of 27 patients (16 men, 11 women; mean age 59.0 ± 13.1 years, range 31 - 83 years) with orbital tumors were enrolled in our study. These 27 patients included 17 patients with benign tumors (cavernous malformation, n = 13; reactive lymphoid hyperplasia, n = 2; meningioma, n = 1; and idiopathic inflammatory pseudotumor, n = 1) and 10 patients with malignant tumors (lymphoma, n = 6; squamous cell carcinoma, n = 2; and adenocarcinoma, n = 2)

2.2. Image acquisition

The MRI examination was performed with a 3.0-T system (Skyra; Siemens Healthcare, Erlangen, Germany) with a 20-channel head and neck coil. Conventional MRI protocol included T2-weighted sequence in axial, coronal and sagittal planes with fat suppression, T1-weighted sequence in axial plane without fat suppression. After contrast agent used, T1-weighted sequence was scanned in axial plane without fat suppression and coronal and sagittal plane with fat suppression.

DWI was obtained by readout-segmented echo planar imaging with the following parameters: acquisition matrix, 224 × 224; field of view, 22 cm; TR, 2310 ms; TE, 91 ms; slice thickness, 3 mm; intersection gap, 0.9 mm; average, 1; echo-spacing, 0.5 ms; and readout segments, 5. Nine different b values (b = 0, 50, 100, 150, 200, 300, 500, 700, and 1000 s/mm^2) were used, with all diffusion-sensitizing gradients applied in 3 orthogonal directions. The total acquisition time was 5 minutes 18 seconds.

DCE-MRI was performed by using 3-dimensional volumetric interpolated breath-hold (3D-VIBE) sequence, with TR/TE = 6.34/2.36 ms, flip angle = 12°, field of view = 18 cm, matrix = 128 × 128, slice thickness = 3 mm, and intersection gap = 0.6 mm. Sixty-five dynamic volumes were acquired consecutively, with a temporal resolution of 5.38 s. On the fifth dynamic volume, 0.1 mmol/kg body weight of gadolinium diethylene triamine pentaacetic acid (Magnevist; Bayer Schering Pharma AG, Berlin, Germany) was intravenously bolus injected via a power injector at a rate of 4 mL/s. The bolus of contrast material was followed by a 20-mL bolus of saline administered at the same injection rate. The total scan time was 5 minutes and 50 seconds.

2.3. Region of interest definition

Regions of interest (ROIs) were drawn on all imaging sections encompassing as much as the tumor area. Visually large necrotic, cystic, and hemorrhagic areas were excluded with reference to the T2-weighted image and contrast-enhanced T1-weighted image. ROIs were slightly smaller in size than tumor size to reduce the influence of partial volume effect.

2.4. Calculation of IVIM-DWI parameters

IVIM-DWI data were transferred from the MRI scanner to an independent personal computer and processed using an in-house software (FireVoxel, CAI^{2}R, New York, NY).[20] The bi-exponential model was fit to the mean signal curve in the ROIs at different b values to calculate the tissue diffusivity (D), pseudo-diffusion coefficient (D^*) and perfusion fraction (f). The IVIM-DWI equation is shown in Eq. (1), in which S_b and S_0 represented the signal intensity with diffusion gradients b and b = 0 s/mm^2, respectively.

$$S_b/S_0 = (1 - f)\, e^{-bD} + f e^{[-b(D*+D)]} \quad (1)$$

A 2-step fitting procedure was implemented to obtain the IVIM-DWI parameters.[9] D was first estimated from a simplified mono-exponential model: $S_b = S_0 \times e^{-bd}$ using data from b value >200/mm^2. This assumes that D^* is significantly greater than D, so that the influence of pseudo-diffusion on signal decay can be neglected for b values >200 s/mm^2. D^* and f were then estimated by nonlinear regression of the bi-exponential function mentioned above using the data from all b values, via keeping D value that estimated from the first step constant.

2.5. Calculation of DCE-MRI parameters

DCE-MRI data were analyzed using in-house software (Omni Kinetics; GE Healthcare, China).[6] For assessing the arterial input function (AIF), 1 ROI was placed manually in the carotid artery ipsilateral to the tumor. The AIF curve was approved by a senior neuro-radiologist to ensure its accuracy. Modified Tofts model was used to calculate the pharmacokinetic parameters, including K^{trans} (volume transfer constant between the plasma and the extracellular extravascular space [EES]), K_{ep} (flux rate constant from EES to blood plasma), and V_e (extravascular extracellular volume fraction).

2.6. Evaluation of inter-reader and intra-reader reproducibility

All above-mentioned quantitative measurements were performed independently by 2 neuro-radiologists (reader 1: with 15 years of experience; reader 2: with 5 years of experience), who were blinded to the study design and clinical information. The measurements of the 2 radiologists were used to assess inter-reader agreement. The average of the 2 measurement results was used for further statistical analysis. For assessing the intra-reader

Table 1

Comparison of IVIM-DWI and DCE-MRI derived parameters between benign and malignant group.

Parameters	Benign group (n = 17)	Malignant group (n = 10)	*P*
D	1.180 ± 0.313	0.657 ± 0.159	<.001
D*	34.975 ± 16.637	61.500 ± 24.051	.002
f	0.168 ± 0.067	0.150 ± 0.034	.430
K^{trans}	0.486 ± 0.312	0.523 ± 0.222	.748
K_{ep}	0.926 ± 0.540	1.372 ± 0.294	.024
V_e	0.548 ± 0.210	0.360 ± 0.149	.021

IVIM-DWI indicates intravoxel incoherent motion diffusion-weighted imaging; DCE-MRI, dynamic contrast-enhanced magnetic resonance imaging; D, tissue diffusivity; D^*, pseudo-diffusion coefficient; f, perfusion fraction; K^{trans}, the volume transfer constant between the plasma and the extracellular extravascular space (EES); V_e, the volume fraction of the EES; K_{ep}, the rate constant from EES to blood plasma.

Numeric data are reported as the mean ± standard deviation.

Unit for D and D^* is 10^{-3} mm^2/s, and Unit for K^{trans} and K_{ep} is min^{-1}.

DCE-MRI = dynamic contrast-enhanced magnetic resonance imaging, DWI = diffusion-weighted imaging, IVIM = intravoxel incoherent motion.

reproducibility, reader 2 was recommended to perform the measurement again, spaced at least 1 month.

2.7. Statistical analysis

Quantitative data were averaged and reported as mean ± standard deviation. Shapiro-Wilk test was used to assess whether the parameters obtained from IVIM-DWI and DCE-MRI were normally distributed because of the small sample size. Independent-sample *t* test was used for the comparison of 6 IVIM-DWI and DCE-MRI derived parameters between benign and malignant group. The significance threshold for difference was set at a *P* value of less than .0083 (0.05/6) for multiple comparison correction. Receiver operating characteristic (ROC) curve analyses were used to assess the diagnostic performance of significant parameters for differentiating orbital malignant from benign tumors. Spearman correlation analyses were used to assess the correlation between parameters obtained from IVIM-DWI and those from DCE-MRI (a correlation coefficient, r, of 0 to 0.5 was defined as a poor correlation, 0.5 to 0.8 was a moderate correlation and >0.8 was considered as a high correlation).[15] Inter-reader and intra-reader reproducibility for these quantitative parameters measured by 2 radiologists were assessed by using intra-class correlation coefficient (ICC). ICC ranged from 0 to 1.00, and values closer to 1.00 represented better reproducibility. The ICC was interpreted as follows: (r < 0.20, poor; r = 0.20–0.40, fair; r = 0.41–0.60, moderate; r = 0.61–0.80, good; r ≧0.81, excellent).[6] Statistical analyses were performed using 2 software packages (SPSS version 20.0, IBM Corp., Armonk, NY; MedCalc 11.4, Mariakerke, Belgium). A *P* value less than .05 was considered to indicate a statistical significance.

3. Results

Table 1 summarizes the IVIM-DWI and DCE-MRI parameters of orbital benign and malignant tumors. Malignant tumors demonstrated significantly lower D (P <.001) and higher D^* (P = .002) than benign tumors. Malignant tumors also showed lower V_e (P = .021) and higher K_{ep} (P = .024) than benign tumors, however the difference did not reach significant after multiple comparison correction. There was no significant difference on f (P = .430) and K^{trans} (P = .748) between benign and malignant tumors (Fig. 1). Representative cases with orbital benign and malignant tumors are shown in Figures 2 and 3.

ROC analyses results indicated that, setting a D value of 0.966×10^{-3} mm^2/s as the cut-off value, optimal diagnostic performance (AUC, 0.888; sensitivity, 100%; specificity, 82.35%) could be obtained for diagnosing malignant tumors. While setting a D^* value of 42.371×10^{-3} mm^2/s as cut-off value, optimal diagnostic performance could be achieved (AUC, 0.847; sensitivity, 90.00%; specificity, 70.59%).

D^* parameter showed poorly positive correlation with K_{ep} (r = 0.427, P = .027), while did not correlate with K^{trans} (r = 0.311, P = 0.114) and V_e (r = −0.159, P = .428). D parameter showed moderately positive correlation with V_e (r = 0.626, P <.001), while did not correlate with K^{trans} (r = 0.247, P = .215) and K_{ep}

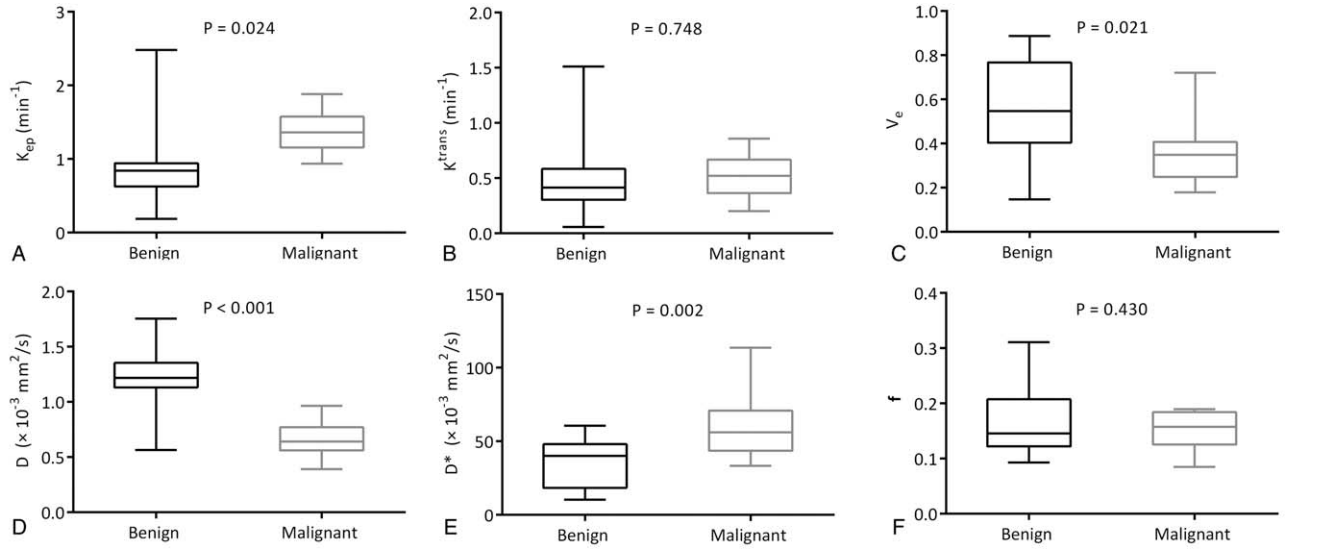

Figure 1. Box plots of K_{ep}, K^{trans}, V_e, D, D^*, and f in orbital benign and malignant tumors. The top and bottom lines of the box represent the 25th to 75th percentile values and the line in the box represents the median value.

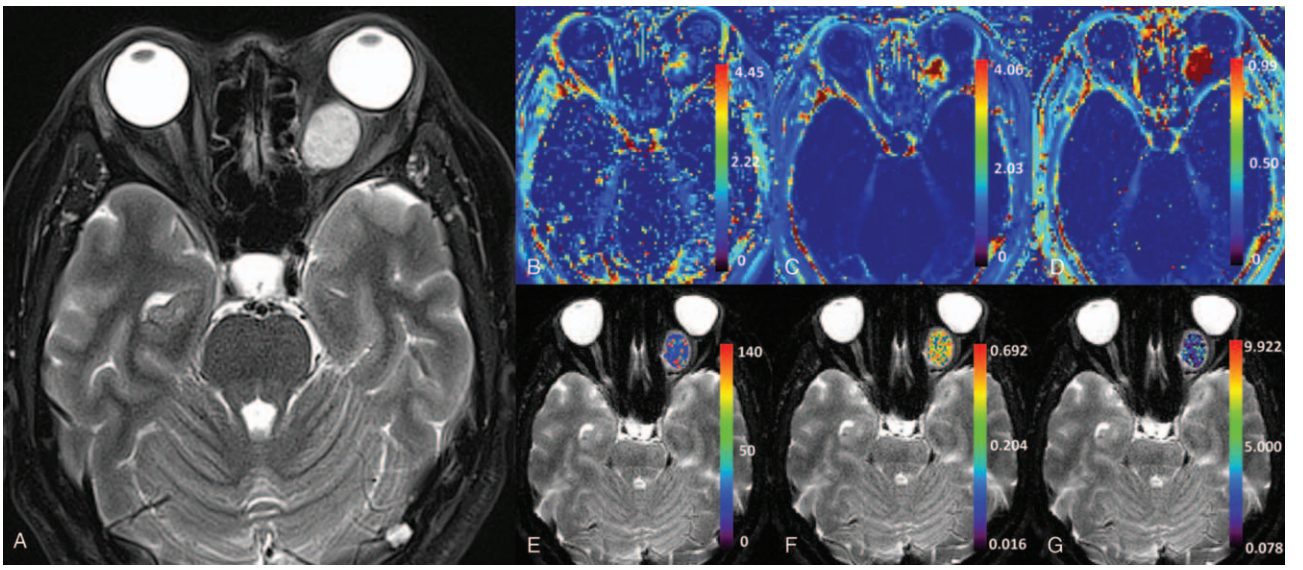

Figure 2. A 54-year-old woman with orbital cavernous malformation. The lesion shows as high signal intensity on T2-weighted image (compared with cerebral cortex) (a). The values for K_{ep}(b), K^{trans} (c), and V_e (d) are 0.956 min^{-1}, 0.725 min^{-1} and 0.771 (upper row), and the values for D (e), D^* (f), and f (g) are 1.284×10^{-3} mm^2/s, $42.371 \times 10^{-3} mm^2/s$ and 0.118 (below row), respectively.

(r = −0.380, P = .050). However, there was no significant correlation found between f and any DCE-MRI parameters (All Ps > .05) (Table 2). The correlations between IVIM-DWI and DCE-MRI parameters are shown with scatter-plot in Figure 4.

Excellent inter-reader (ICCs of 0.921 for D, ICC of 0.837 for D^*, ICC of 0.891 for f, ICC of 0.953 for K^{trans}, ICC of 0.958 for K_{ep}, and ICC of 0.962 for V_e) and intra-reader (ICCs of 0.936 for D, ICC of 0.836 for D^*, ICC of 0.896 for f, ICC of 0.947 for K^{trans}, ICC of 0.962 for K_{ep}, and ICC of 0.957 for V_e) reproducibility was achieved for the measurements of IVIM-DWI and DCE-MRI parameters.

4. Discussion

Our study had several main findings. First, orbital malignant tumors showed significantly lower D and higher D^* compared with benign tumors, while f did not differ significantly between 2 groups. Second, poor to moderate correlations were found between IVIM-DWI and DCE-MRI parameters. D^* showed poorly positive correlation with K_{ep}, meanwhile D showed moderately positive correlation with V_e. To the best of acknowledge, our study was the first one which used IVIM-DWI for assessing orbital tumors and meanwhile assessed the

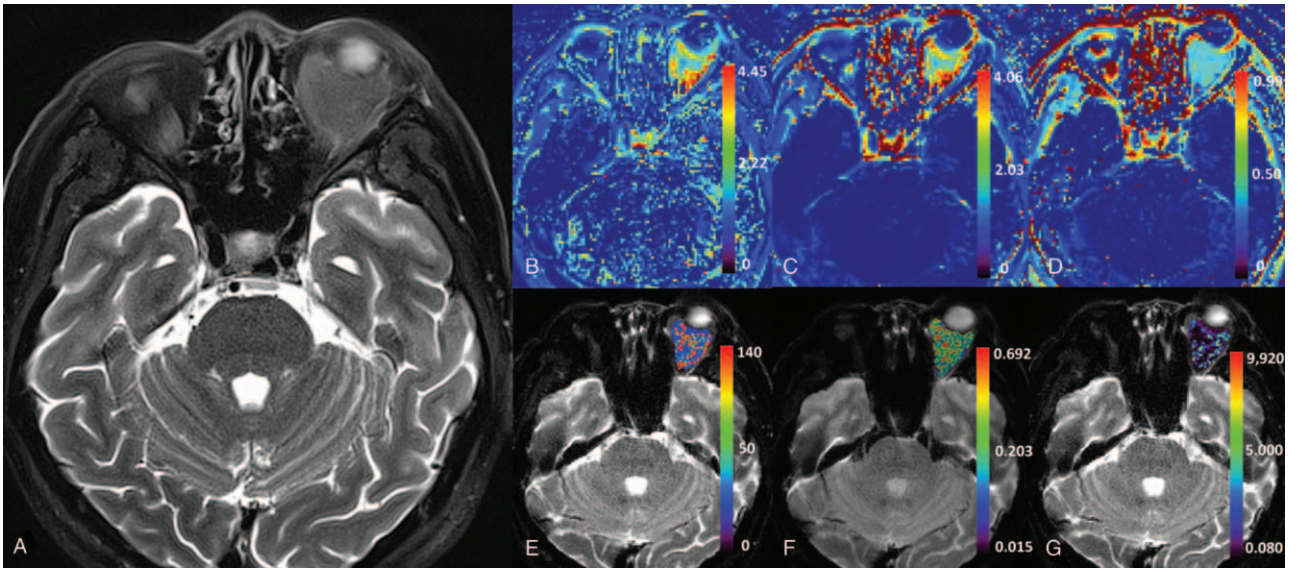

Figure 3. A 69-year-old man with orbital lymphoma. The lesion shows as low signal intensity on T2-weighted image (compared with cerebral cortex) (a). The values for K_{ep}(b), K^{trans} (c), and V_e (d) are 1.576 min^{-1}, 0.504 min^{-1}, and 0.321 (upper row), and the values for D (e), D^* (f), and f (g) are $0.538 \times 10^{-3} mm^2/s$, 61.405×10^{-3} mm^2/s and 0.126 (below row), respectively.

Table 2

Correlation between parameters from IVIM-DWI and those from DCE-MRI.

	D		D*		f	
Parameters	**r**	***P***	**R**	***P***	**r**	***P***
K^{trans}	0.247	.215	0.311	.114	−0.214	.283
K_{ep}	−0.380	.050	0.427	.027*	−0.225	.259
V_e	0.626	<.001*	−0.159	.428	−0.036	.860

IVIM-DWI indicates intravoxel incoherent motion diffusion-weighted imaging; DCE-MRI, dynamic contrast-enhanced magnetic resonance imaging; D, tissue diffusivity; D*, pseudo-diffusion coefficient; f, perfusion fraction; K^{trans}, the volume transfer constant between the plasma and the extracellular extravascular space (EES); V_e, the volume fraction of the EES; K_{ep}, the rate constant from EES to blood plasma.
* indicates the statistically significant *P* values.
DCE-MRI = dynamic contrast-enhanced magnetic resonance imaging, DWI = diffusion-weighted imaging, IVIM = intravoxel incoherent motion.

correlation between IVIM-DWI and DCE-MRI parameters in orbital tumors.

Malignant orbital tumors demonstrated significantly lower D than benign tumors in our study, which was consistent with previous studies based on conventional DWI using 2 b values.[1,3–7] The increased cellularity within malignant tumors would decrease water diffusivity, subsequently, D would decrease. D*, which was reported to be proportional to the mean capillary segment length and average blood velocity, was usually viewed as an indicator of tumor micro-vessel attenuation.[21] One prior study indicated that D* was significantly higher in malignant lymph nodes than that in benign lymph nodes.[22] In our study, malignant orbital tumors also showed higher D* than benign tumors. Present result indicated that D* could reflect the tumor vascularity and serve as an effective biomarker for differentiating orbital tumors.

f, which was determined as the signal intensity ratio of blood capillaries and tumor tissues, might be an indicator of vascular permeability.[21] During the analysis of f parameter, all relaxation effects were ignored. This was acceptable as long as the relaxation times of tissue and capillary blood were similar. However, T2 contributions from tumor tissues and blood capillaries might be greatly different. It was well known that the T2 of tumor tissue tended to increase. In our study, the majority within benign group were cavernous malformation whose T2 was similar with blood capillaries. However, in malignant group, prolonged T2 of the

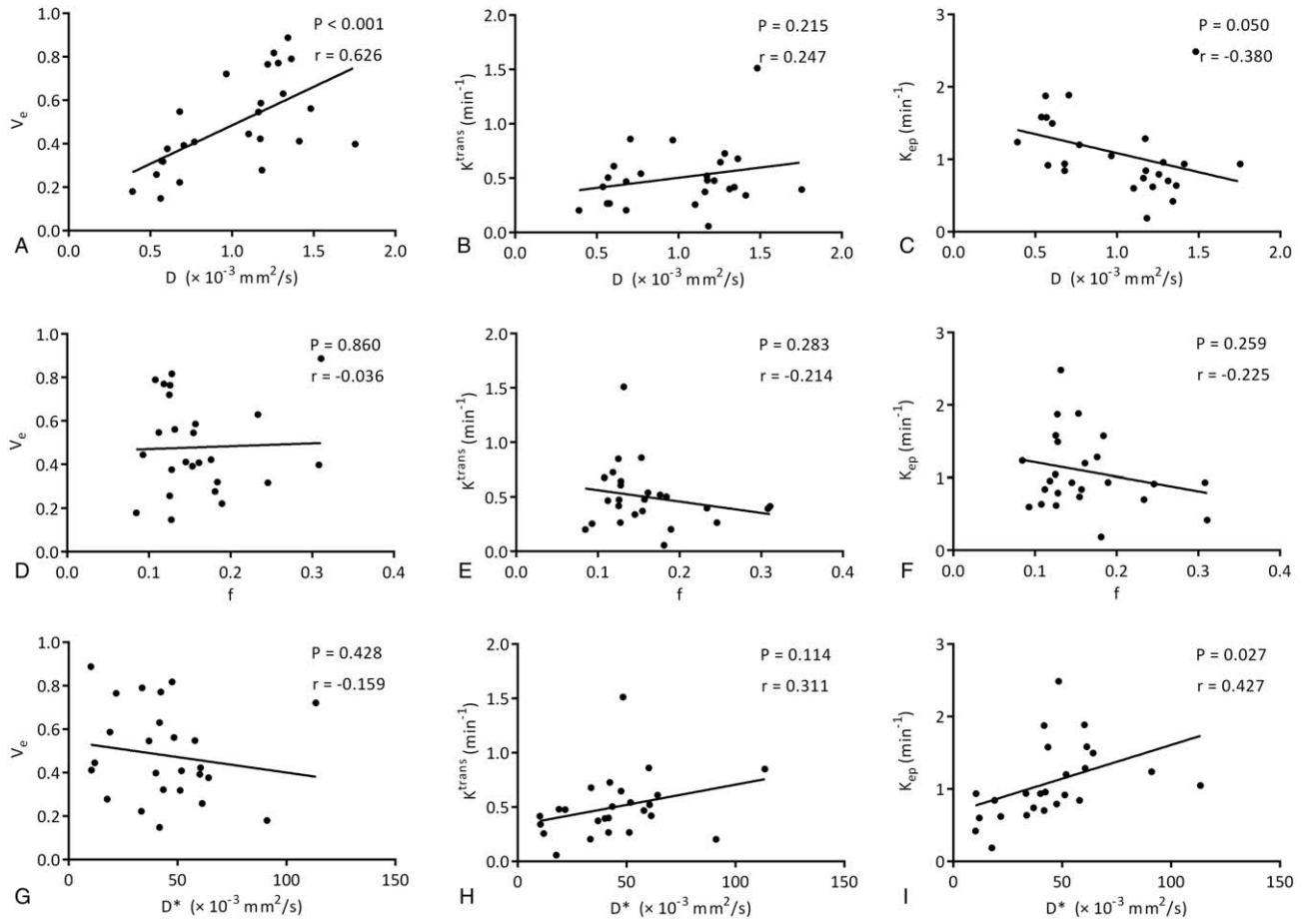

Figure 4. Scatter plots show the correlations of quantitative parameters between IVIM-DWI and DCE-MRI. Spearman correlation coefficient (r) and *P* value are showed in each scatter plot. DCE-MRI = dynamic contrast-enhanced magnetic resonance imaging, DWI = diffusion-weighted imaging, IVIM = intravoxel incoherent motion.

tumor tissue would lead to a lower calculated f value.[23] Therefore, f did not differed significantly between benign and malignant orbital tumors. This results indicated that the interpretation of f in tumors should be performed carefully because of the T2 contribution.

Previous study indicated that orbital malignant tumors showed significantly higher K_{ep} and lower V_e than benign mimics.[4] Lower V_e in malignant tumors might be associated with the hypercellularity and limited EES, while higher K_{ep} might be associated with the limited EES and earlier flux of contrast from EES to blood plasma.[4] In present study, malignant tumors also showed lower V_e and higher K_{ep} than benign tumors, however, the difference was not significant after multiple comparison correction. This result might be associated with the different pathological composition and limited sample size in our study cohort.

The correlation between IVIM-DWI and DCE-MRI derived parameters had been investigated in various organs and pathologies, [14–19,21] however no consistent results were obtained. Jia et al reported that f correlated significantly with the enhancement amplitude and maximum slope of increase semi-quantitatively derived from DCE-MRI in nasopharyngeal carcinoma.[21] However, Bisdas et al indicated no evident correlation between IVIM-DWI and DCE-MRI in cerebral glioma.[16] In our study, although significant correlations existed between D^* and K_{ep}, and D and V_e, the correlations were only poor or moderate. Possible explanations for the discrepancy among published studies and our study might be:

(1) IVIM-DWI directly measured microscopic translational motions associated with microcirculation in small vessels. However, it should be considered that the diffusion signal could be influenced by any flow phenomena apart from blood flow, such as cerebrospinal fluid flow in the brain.[9,15–17]
(2) DCE-MRI measured the tissue perfusion based on the uptake, extravasation, and removal of contrast medium, however, this process was tissue-specific.[17]

Different tissues might demonstrated different hemodynamics characteristic. Further study was needed to clarify how IVIM-DWI and DCE-MRI influenced by the physiological characteristic in different functional tissues.

Besides the limited sample size, our study had some other limitations. First, we included orbital cavernous malformation in our study cohort. Its pathological structure was different from other tumors. Whether the theory of IVIM-DWI and DCE-MRI are suitable for cavernous malformation or not is still unknown. Second, we usually could make an accurate diagnosis for some orbital tumors just based on the image features on routine MR images. In clinical setting, accurate differentiation between benign and malignant lymphoproliferative disorders was more difficult. Further study focusing on orbital lymphoproliferative disorders, and assessing the added value of IVIM-DWI to routine MR image features in the differentiation would be more valuable. Third, previous study indicated that IVIM-DWI parameters, especially D^*, was easily influenced by the involuntary motion such as the cardiac cycle.[24] However, effective cardiography triggering was not performed during IVIM-DWI scan. Last, we did not correlate the perfusion parameters derived from IVIM-DWI and DCE-MRI with the angiogenesis-related biomarkers. Further study focusing on this subject would be valuable for clarifying the histopathological meanings of IVIM-DWI and DCE-MRI.

In conclusion, our study showed that IVIM-DWI might be a potential useful adjunctive perfusion technique for differentiating orbital tumors, D and D^* were potential discriminating imaging-biomarkers. Poor to moderate correlations were found between IVIM-DWI and DCE-MRI derived parameters. Further investigations including measurement of angiogenesis-related biomarkers were warranted for clarifying the relationship between IVIM-DWI and DCE-MRI in orbital tumors.

Author contributions

Conceptualization: Hu Liu, Fei-Yun Wu, Hai-Bin Shi.
Data curation: Xiao-Quan Xu.
Formal analysis: Xiao-Quan Xu.
Investigation: Xiao-Quan Xu, Fei-Yun Wu, Hai-Bin Shi.
Methodology: Xiao-Quan Xu, Hao Hu, Guo-Yi Su, Hai-Bin Shi.
Software: Xiao-Quan Xu, Fei-Yun Wu.
Supervision: Fei-Yun Wu, Hai-Bin Shi.
Validation: Xiao-Quan Xu, Fei-Yun Wu, Hai-Bin Shi.
Writing – original draft: Xiao-Quan Xu.
Writing – review & editing: Fei-Yun Wu, Hai-Bin Shi.

References

[1] Xu XQ, Hu H, Su GY, et al. Orbital indeterminate lesions in adults: combined magnetic resonance morphometry and histogram analysis of apparent diffusion coefficient maps for predicting malignancy. Acad Radiol 2016;23:200–8.
[2] Xian J, Zhang Z, Wang Z, et al. Value of MR imaging in the differentiation of benign and malignant orbital tumors in adults. Eur Radiol 2010;20:1692–702.
[3] Sepahdari AR, Aakalu VK, Setabutr P, et al. Indeterminate orbital masses: restricted diffusion at MR imaging with echo-planar diffusion-weighted imaging predicts malignancy. Radiology 2010;256:554–64.
[4] Xu XQ, Qian W, Ma G, et al. Combined diffusion-weighted imaging and dynamic contrast-enhanced MRI for differentiating radiologically indeterminate malignant from benign orbital masses. Clin Radiol 2017;72:903.e9–15.
[5] Ro SR, Asbach P, Siebert E, et al. Characterization of orbital masses by multiparametric MRI. Eur J Radiol 2016;85:324–36.
[6] Xu XQ, Hu H, Liu H, et al. Benign and malignant orbital lymphoproliferative disorders: differentiating using multiparametric MRI at 3.0T. J Magn Reson Imaging 2017;45:167–76.
[7] Sun B, Song L, Wang X, et al. Lymphoma and inflammation in the orbit: diagnostic performance with diffusion-weighted imaging and dynamic contrast-enhanced MRI. J Magn Reson Imaging 2017;45:1438–45.
[8] Gaddikeri S, Gaddikeri RS, Tailor T, et al. Dynamic contrast-enhanced MR imaging in head and neck cancer: techniques and clinical applications. AJNR Am J Neuroradiol 2016;37:588–95.
[9] Xu XQ, Choi YJ, Sung YS, et al. Intravoxel incoherent motion MR imaging in the head and neck: correlation with dynamic contrast-enhanced MR imaging and diffusion-weighted imaging. Korean J Radiol 2016;17:641–9.
[10] Sumi M, Nakamura T. Head and neck tumours: combined MRI assessment based on IVIM and TIC analyses for the differentiation of tumors of different histological types. Eur Radiol 2014;24:223–31.
[11] Sumi M, Nakamura T. Head and neck tumors: assessment of perfusion-related parameters and diffusion coefficients based on the intravoxel incoherent motion model. AJNR Am J Neuroradiol 2013;34:410–6.
[12] Paudyal R, Oh JH, Riaz N, et al. Intravoxel incoherent motion diffusion-weighted MRI during chemoradiation therapy to characterizeand monitor treatment response in human papillomavirus head and neck squamous cell carcinoma. J Magn Reson Imaging 2017;45:1013–23.
[13] Lecler A, Savatovsky J, Balvay D, et al. Repeatability of apparent diffusion coefficient and intravoxel incoherent motion parameters at 3.0 Tesla in orbital lesions. Eur Radiol 2017;27:5094–103.
[14] Hectors SJ, Wagner M, Besa C, et al. Intravoxel incoherent motion diffusion-weighted imaging of hepatocellular carcinoma: Is there a correlation with flow and perfusion metrics obtained with dynamic contrast-enhanced MRI. J Magn Reson Imaging 2016;44:856–64.
[15] Liu C, Wang K, Chan Q, et al. Intravoxel incoherent motion MR imaging for breast lesions: comparison and correlation with pharmacokinetic evaluation from dynamic contrast-enhanced MR imaging. Eur Radiol 2016;26:3888–98.

[16] Marzi S, Stefanetti L, Sperati F, et al. Relationship between diffusion parameters derived from intravoxel incoherent motion MRI and perfusion measured by dynamic contrast-enhanced MRI of soft tissue tumors. NMR Biomed 2016;29:6–14.
[17] Wang LL, Lin J, Liu K, et al. Intravoxel incoherent motion diffusion-weighted MR imaging in differentiation of lung cancer from obstructive lung consolidation: comparison and correlation with pharmacokinetic analysis from dynamic contrast-enhanced MR imaging. Eur Radiol 2014;24:1914–22.
[18] Marzi S, Piludu F, Forina C, et al. Correlation study between intravoxel incoherent motion MRI and dynamic contrast-enhanced MRI in head and neck squamous cell carcinoma: evaluation in primary tumors and metastatic nodes. Magn Reson Imaging 2017;37:1–8.
[19] Fujima N, Yoshida D, Sakashita T, et al. Intravoxel incoherent motion diffusion-weighted imaging in head and neck squamous cell carcinoma: assessment of perfusion-related parameters compared to dynamic contrast-enhanced MRI. Magn Reson Imaging 2014;32: 1206–13.
[20] Xu X, Su G, Hu H, et al. Effects of regions of interest methods on apparent coefficient measurement of the parotid gland in early Sjögren's syndrome at 3T MRI. Acta Radiol 2017;58:27–33.
[21] Jia QJ, Zhang SX, Chen WB, et al. Initial experience of correlating parameters of intravoxel incoherent motion and dynamic contrast-enhanced magnetic resonance imaging at 3.0 T in nasopharyngeal carcinoma. Eur Radiol 2014;24:3076–87.
[22] Liang L, Luo X, Lian Z, et al. Lymph node metastasis in head and neck squamous carcinoma: Efficacy of intravoxel incoherent motion magnetic resonance imaging for the differential diagnosis. Eur J Radiol 2017;90: 159–65.
[23] Sumi M, Van Cauteren M, Sumi T, et al. Salivary gland tumors: use of intravoxel incoherent motion MR imaging for assessment of diffusion and perfusion for the differentiation of benign from malignant tumors. Radiology 2012;263:770–7.
[24] Federau C, Hagmann P, Maeder P, et al. Dependence of brain intravoxel incoherent motion perfusion parameters on the cardiac cycle. PLoS One 2013;8:e72856.